Results from Super-Kamiokande

Takaaki Kajita[a] *

[a]Research Center for Cosmic Neutrinos[1] and Kamioka Observatory[2],
Institute for Cosmic Ray Research, Univ. of Tokyo
[1]Midori-cho 3-2-1, Tanashi-shi, Tokyo 188-8502, Japan
[2]Higashi-Mozumi, Kamioka-cho, Gifu, 506-1205, Japan
for the Super-Kamiokande collaboration

Results from Super-Kamiokande on atmospheric neutrinos and solar neutrinos are presented. The atmospheric neutrino data exhibited a zenith angle dependent deficit of muon neutrinos. Experimental biases and uncertainties in the prediction were unable to explain the data. However, the data were in good agreement with two flavor $\nu_\mu \leftrightarrow \nu_\tau$ oscillations. The solar neutrino data showed a deficit of the neutrinos. The day-night effect and the energy spectrum of recoil electrons were studied.

1. Introduction

It has been known that the observed solar and atmospheric neutrino data disagree with the theoretical predictions. Neutrino oscillations were quoted as the explanations to these data. In 1998, Super-Kamiokande obtained a clear answer to the atmospheric neutrino problem. The data showed a zenith-angle dependent deficit of μ-like events. While uncertainties in the flux prediction, cross sections and experimental biases were ruled out, the data were in good agreement with $\nu_\mu \leftrightarrow \nu_\tau$ oscillations.

Super-Kamiokande is a large water Cherenkov detector. It is located in Kamioka Observatory, 1000 m below the peak of Mt. Ikenoyama, Kamioka, Japan. 50 kton of pure water is contained in a stainless steel tank of 39.3 meters in diameter and 41.4 m in height. The detector is optically separated into two regions, the inner and outer detectors. The inner detector has 36.2 m in height and 33.8 m in diameter. The outer detector, which has the thickness of 2.6 to 2.75 m (including an insensitive region of 0.55 m thickness), completely surrounds the inner detector. About 11,000 and 1,900 Photo Multiplier Tubes (PMTs) are instrumented to detect Cherenkov photons for inner and outer detectors, respectively. The 1000 m of rock over the detector makes it possible to study relatively rare events such as solar neutrinos and atmospheric neutrinos.

In this paper, results from Super-Kamiokande on atmospheric neutrinos and solar neutrinos are presented. The data described in this paper are slightly updated from those presented at the conference.

2. Atmospheric neutrinos

Cosmic ray interactions in the atmosphere produce neutrinos. The prediction of the absolute flux has an uncertainty of about $\pm 20\%$. However, the flavor ratio of the atmospheric neutrino flux, $(\nu_\mu + \bar{\nu}_\mu)/(\nu_e + \bar{\nu}_e)$, has been calculated to an accuracy of better than 5% in a broad energy range from 0.1 GeV to higher than 10 GeV. The calculated flux ratio has a value of about 2 for energies $\lesssim$1GeV and increases with increasing neutrino energy. The fluxes of upward and downward going neutrinos are expected to be nearly equal for $E_\nu >$(a few GeV), above which effects due to the geomagnetic field on cosmic rays are small.

The $(\nu_\mu + \bar{\nu}_\mu)/(\nu_e + \bar{\nu}_e)$ flux ratio has been measured in deep underground experiments by observing final-state leptons produced by charged-current interactions of neutrinos on nuclei. The measurements are reported as $R \equiv (\mu/e)_{data}/(\mu/e)_{MC}$, where μ and e are the num-

*This work was partly supported by the Japanese Ministry of Education, Science, Sports and Culture.

ber of muon-like (μ-like) and electron-like (e-like) events observed in the detector for both data and Monte Carlo (MC) simulation. This ratio largely cancels experimental and theoretical uncertainties, especially the uncertainty in the absolute flux. The observed values of R by Kamiokande [1], [2] were significantly smaller than unity for both below and above 1 GeV energy ranges. Consistent results were obtained by IMB-3(<1.5GeV) [3] and Soudan-2 [4]. Neutrino oscillations have been suggested to explain the small values of R.

For detectors near the surface of the Earth, the neutrino flight distance, and thus the oscillation probability, is a function of the zenith angle of the neutrino direction. The zenith angle dependence of the neutrino flux measured by Kamiokande [2] at high energies, together with the small R values, has been cited as evidence for neutrino oscillations. Based on these measurements, Kamiokande obtained the allowed parameter regions of neutrino oscillations. Because of the relatively small statistics, both $\nu_\mu \leftrightarrow \nu_e$ and $\nu_\mu \leftrightarrow \nu_\tau$ oscillations were allowed. Recently, a long baseline reactor experiment, CHOOZ [5], excluded the $\nu_\mu \leftrightarrow \nu_e$ solution of the atmospheric neutrino problem.

In 1998, Super-Kamiokande reported that the atmospheric neutrino data gave evidence for neutrino oscillations [7]. After that, the statistics of the Super-Kamiokande data were increased by 60 to 80% depending of the data sample. Also, some Monte Carlo parameters were updated [2] . Results based on the updated data samples and updated Monte Carlo are presented here.

2.1. Fully and partially contained events

Super-Kamiokande observed a total of 6791 fully-contained (FC) events and 470 partially-contained (PC) events in a 52 kton·year exposure. FC events deposit all of their Cherenkov light in the inner detector, while PC events have exiting tracks which deposit some Cherenkov light in the outer detector. The neutrino interaction vertex was required to have been reconstructed within the 22.5 kiloton fiducial volume, defined to be > 2 m from the PMT wall. The number of FC+PC events observed so far in Super-Kamiokande was more than 6 times larger than that in Kamiokande.

	Data	MC
Sub-GeV		
e-like	1826	1754
μ-like	1852	2618
$R = 0.68 \pm 0.02 \pm 0.05$		
Multi-GeV		
e-like	439	414
μ-like(FC+PC)	821	1143
$R = 0.68 \pm 0.04 \pm 0.08$		

Table 1
Summary of the atmospheric $(\mu/e)_{data}/(\mu/e)_{MC}$ ($\equiv R$) ratio measurement.

For the analysis of FC events, only single-ring events were used. Single-ring events were identified as e-like or μ-like based on a likelihood analysis of light detected around the Cherenkov cone. The probability of misidentification of particle type was estimated to be less than 1%. The FC events were separated into "sub-GeV" ($E_{vis} <$ 1330 MeV) and "multi-GeV" ($E_{vis} >$ 1330 MeV) samples, where E_{vis} was defined to be the energy of an electron that would produce the observed amount of Cherenkov light. E_{vis} = 1330 MeV corresponds to ~1400 MeV/c for muons.

In a full MC simulation, 87% (95%) of the sub-GeV e-like (μ-like) events were ν_e (ν_μ) charged-current (CC) interactions and 80% (99%) of the multi-GeV e-like (μ-like) events were ν_e (ν_μ) CC interactions. PC events were estimated to be 97% ν_μ CC interactions; hence, all PC events were classified as μ-like, and no single-ring and particle identification requirements were made [6].

The numbers of observed and predicted events for the sub- and multi-GeV energy regions in Super-Kamiokande are summarized in Table 1. Significantly small values of R in both the sub-GeV and multi-GeV samples were observed. Sev-

[2] Among the updated parameters, the most important one is the use of GRV94 [8] parton distribution function. The event rate of the present Monte Carlo is higher than that used in Ref. [6,7].

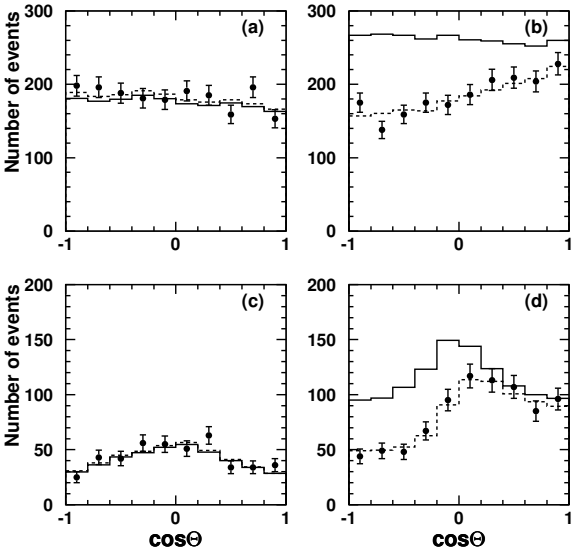

Figure 1. Zenith angle distributions observed in Super-Kamiokande for (a) sub-GeV e-like, (b) sub-GeV μ-like, (c) multi-GeV e-like and (d) multi-GeV (FC+PC) μ-like events. CosΘ =1 means down-going particles. The solid histograms show the MC prediction for the no neutrino oscillation case. The dashed histograms show the MC prediction for $\nu_\mu \leftrightarrow \nu_\tau$ oscillations with $\sin^2 2\theta$ =1 and Δm^2 =3.5×10^{-3} eV^2. In the oscillation histograms, the absolute normalization was adjusted to get the minimum χ^2.

eral sources of systematic uncertainties in these measurements were considered [6]. For the sub-GeV(multi-GeV) sample, the total systematic uncertainty in R was 8(12)%.

The zenith angle distributions for the sub- and multi-GeV samples are shown in Figure 1. The μ-like data from Super-Kamiokande exhibited a strong up-down asymmetry in zenith angle (Θ) while no significant asymmetry was observed in the e-like data. For further description of the data, we define up-down ratio, U/D, where U is the number of upward-going events ($-1 < \cos\Theta < -0.2$) and D is the number of downward-going events ($0.2 < \cos\Theta < 1$). The ratio is expected to be near unity independent of flux model for $E_\nu > 1$ GeV, above which effects due to the Earth's magnetic field on cosmic rays are small.

Table 2 summarizes the U/D values observed in Super-Kamiokande. U/D for e-like events were consistent with expectations. U/D for high momentum μ-like events significantly deviated from unity, while U/D for low momentum μ-like events was consistent with unity. The average angle between the final state lepton direction and the incoming neutrino direction is 55° at p = 400 MeV/c and 20° at 1.5 GeV/c. Hence, at the momentum range below 400 MeV/c, the possible up-down asymmetry of the neutrino flux is largely washed out.

The U/D value from Super-Kamiokande for the multi-GeV FC+PC μ-like events, $0.52\ ^{+0.05}_{-0.04} \pm 0.006$, deviated from unity by 8 standard deviations. The Kamiokande U/D value for the multi-GeV FC+PC μ-like events, $0.58\ ^{+0.13}_{-0.12}$ [2], was consistent with this value. These numbers, which are close to 0.5, suggest a near maximal neutrino mixing.

Based on these data, we have examined the hypotheses of two-flavor $\nu_\mu \leftrightarrow \nu_e$ and $\nu_\mu \leftrightarrow \nu_\tau$ oscillations by a χ^2 method [7]:

$$\chi^2 = \sum_{cos\Theta,p}^{70} \left(\frac{N_{Data} - N_{MC}(\sin^2 2\theta, \Delta m^2, \epsilon_j)}{\sigma} \right)^2 + \sum_j \left(\frac{\epsilon_j}{\sigma_j} \right)^2,$$

where the sum is over five bins equally spaced in $\cos\Theta$ and seven momentum bins for both e-like events and μ-like plus PC events (70 bins total). The statistical error, σ, accounts for both data statistics and the weighted MC statistics. N_{Data} is the measured number of events in each bin. $N_{MC}(\sin^2 2\theta, \Delta m^2, \epsilon_j)$ is the expected number of MC events and is a function of $\sin^2 2\theta$, Δm^2 and ϵ_j. ϵ_j are parameters which are related to the systematic uncertainties. The parameters (and their uncertainties, σ_j) considered in this analysis are: overall normalization (25%, but this was fitted as a free parameter), E_ν spectral index (0.05), sub-GeV R (8%), multi-GeV R (12%), relative normalization of PC to FC (8%), L/E_ν (15%),

	e-like		μ-like	
	Data	MC	Data	MC
Sub-GeV, <400MeV/c	$1.10^{+0.08}_{-0.08} \pm 0.01$	1.04±0.02±0.03	$0.98^{+0.09}_{-0.08} \pm 0.002$	1.04±0.02±0.02
Sub-GeV, >400MeV/c	$1.10^{+0.09}_{-0.08} \pm 0.01$	1.09±0.02±0.03	$0.65^{+0.05}_{-0.04} \pm 0.002$	1.03±0.02±0.02
Multi-GeV	$0.99^{+0.12}_{-0.10} \pm 0.01$	1.04±0.03±0.03	$0.52^{+0.05}_{-0.04} \pm 0.006$	0.99±0.02±0.02

Table 2
Summary of the up/down ratio, U/D, for e-like and μ-like events from Super-Kamiokande. For multi-GeV μ-like, both FC and PC events are included.

sub-GeV (2.4%) and multi-GeV (2.7%) up-down ratios. In, Figure 1, the zenith-angle distribution of the data are compared to the MC expectation (no oscillations, solid histograms) and the best-fit expectation for $\nu_\mu \leftrightarrow \nu_\tau$ oscillations (dashed histograms). The oscillated MC well reproduced the zenith angle distributions of the data. The 90% C.L. allowed region is shown in Figure 2.

For the test of $\nu_\mu \leftrightarrow \nu_e$ oscillations, the Super-Kamiokande data resulted in a relatively poor fit due to the non-observation of excess of upward-going e-like events (especially in the multi-GeV energy region), see Figure 1. We concluded that the $\nu_\mu \leftrightarrow \nu_e$ hypothesis was not favored. This result was consistent with that from CHOOZ [5].

2.2. Upward going muons

Energetic atmospheric ν_μ's passing through the Earth interact with rock surrounding the detector and produce muons via CC interactions. These neutrino events are observed as upward going muons. Upward going muons are categorized into two types. One is "upward through-going muons" which enter into the detector and exit, and the other is "upward stopping muons" which enter into the detector and stop in the detector.

Super-Kamiokande observed 1028 upward through-going muon events (including 7 estimated background events) during 923 detector live days. The observed flux of upward through-going muons was $1.70 \pm 0.05(stat.) \pm 0.02(sys.) \times 10^{-13} cm^{-2} sec^{-1} sr^{-1}$. The expected flux based on the calculated flux of Ref. [10] was $1.97 \pm 0.44(theo.) \times 10^{-13} cm^{-2} sec^{-1} sr^{-1}$. Figure 3 shows the zenith-angle distribution of the upward through-going muon flux observed in Super-Kamiokande. The prediction had a flatter zenith-angle distribution than the data. A χ^2 comparison of the data and MC shapes gave a relatively large value, 24.7/9 DOF.

The $\nu_\mu \leftrightarrow \nu_\tau$ oscillation hypothesis was tested by a χ^2 method [9]:

$$\chi^2 = \sum_{cos\Theta}^{10} \left(\frac{\phi_{Data} - \alpha \cdot \phi_{MC}(\sin^2 2\theta, \Delta m^2)}{\sigma} \right)^2 + \left(\frac{\alpha - 1}{\sigma_\alpha} \right)^2,$$

where σ is the statistical and systematic error in the observed flux (ϕ_{Data}) and α and σ_α are an absolute normalization factor of the expected flux($\phi_{MC}(\sin^2 2\theta, \Delta m^2)$) and its uncertainty, respectively. σ_α was taken to be ±22% by adding the theoretical uncertainty and correlated experimental errors. The uncertainty in the absolute neutrino flux (±20%) was the dominant source of σ_α. A minimum χ^2 was calculated by changing α for each ($\sin^2 2\theta$, Δm^2).

χ^2_{min} occurred at $(\sin^2 2\theta, \Delta m^2) = (0.77, 1.4 \times 10^{-3}$ eV$^2)$ with α =1.12. The χ^2_{min} value was 11.6/8 DOF. The allowed regions did not change significantly for two assumptions of the neutrino flux [10],[11]. Figure 2 shows the allowed regions obtained from these upward through-going muon data. The allowed region obtained by the upward through-going muon data from Kamiokande is also shown [12]. These allowed regions are larger than those of contained events. But they overlap the allowed regions obtained by the contained data.

Because of the large detector dimension of

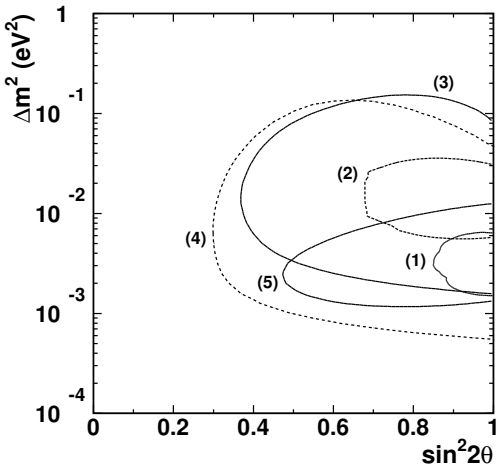

Figure 2. The allowed parameter regions of $\nu_\mu \leftrightarrow \nu_\tau$ neutrino oscillations obtained by Super-Kamiokande and Kamiokande. Inside of each curve is allowed at 90% C.L.. (1) and (2) show the regions obtained by contained event analyses from Super-Kamiokande and Kamiokande, respectively. (3) and (4) show the regions obtained by upward through-going muons from Super-Kamiokande and Kamiokande, respectively. (5) shows the region obtained by the (stopping/trough-going) ratio analysis of upward going muons from Super-Kamiokande.

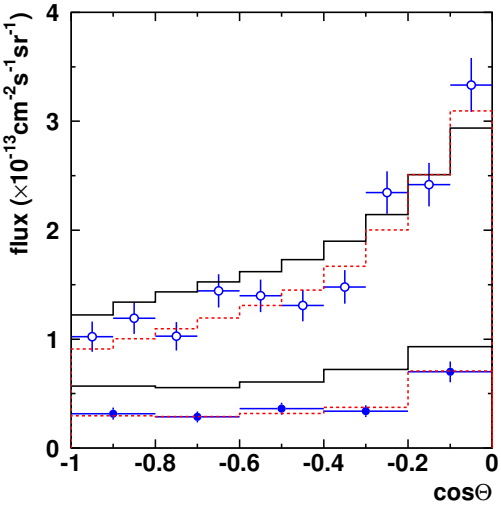

Figure 3. Zenith angle distribution of upward-going muon flux observed in Super-Kamiokande. Blank (filled) circles with error bars show the upward through-going (stopping) muon data and the histograms show the corresponding predictions. Error bars show statistical + uncorrelated experimental systematic errors. Estimated backgrounds are subtracted. The solid histograms show the expected fluxes for the null neutrino oscillation case. The dashed histograms show the expected fluxes for the $\nu_\mu \leftrightarrow \nu_\tau$ oscillation case with $\sin^2 2\theta$ =1.0, $\Delta m^2 = 3.5 \times 10^{-3}$ eV^2.

Super-Kamiokande, a substantial fraction of upward going muons stop in the detector. The mean neutrino energy of the upward stopping muons is about 10GeV, which is substantially lower than that of the upward through-going muons (∼100 GeV). Therefore, in some neutrino oscillation parameters, it is expected that an observed (stopping/through-going) flux ratio of upward going muons is different from the calculated ratio.

Super-Kamiokande observed 245 upward stopping muons (including 23 estimated background events) during 902 detector live days. Figure 3 shows the zenith angle distribution of the upward stopping muon flux. Also shown in the same figure are the predicted fluxes with and without neutrino oscillations. Clearly, the predicted distribution with neutrino oscillations agrees well with the data within the uncertainty of the absolute normalization (±22%). The (stopping/through-going) flux ratio (≡ $\Re$) was calculated. The observed value was $\Re$ =$0.235 \pm 0.018(stat.)^{+0.013}_{-0.011}(sys.)$, while the predicted value was $\Re$ =$0.37^{+0.049}_{-0.044}(theo.)$. The observed value was 2.8σ smaller than the prediction.

The 90% C.L. allowed region of the neutrino oscillation parameters was estimated by a χ^2 test [13]:

$$\chi^2 = \sum_{cos\Theta}^{5} \left(\frac{\Re_{Data} - \beta \cdot \Re_{MC}(\sin^2 2\theta, \Delta m^2)}{\sigma} \right)^2$$

$$+\left(\frac{\beta-1}{\sigma_\beta}\right)^2,$$

where σ is the experimental (mostly statistical) error in the observed ratio ($\Re_{Data}$) and β and σ_β are an uncertainty factor of the expected ratio ($\Re_{MC}(\sin^2 2\theta, \Delta m^2)$) and its 1 σ error, respectively. σ_β was taken to be $\pm 14\%$ by adding the theoretical uncertainty and correlated experimental systematic errors.

Figure 2 shows the allowed region obtained from this analysis. Again, the allowed region is larger than those of contained events. But it overlaps the allowed regions obtained by the contained and upward through-going muon data.

Finally, since the contained events and upward-going muon events consistently suggested the neutrino oscillations in the same parameter region, an allowed region was obtained by combining all the atmospheric neutrino data from Super-Kamiokande. The allowed region (together with the allowed region obtained by Kamiokande [12] in a similar analysis) is shown in Figure 4 [14]. The χ^2 value of the neutrino oscillation analysis[3] was 67.5/82 DOF at the best fit point (3.5×10^{-3}eV^2, 1.0). Even if we extended the analysis to the unphysical region of $\sin^2 2\theta > 1$, the best fit point was the same. The 90% C.L. allowed region of the oscillation parameters was; $2\times10^{-3} < \Delta m^2 < 6\times10^{-3}$eV^2 and $\sin^2 2\theta > 0.84$.

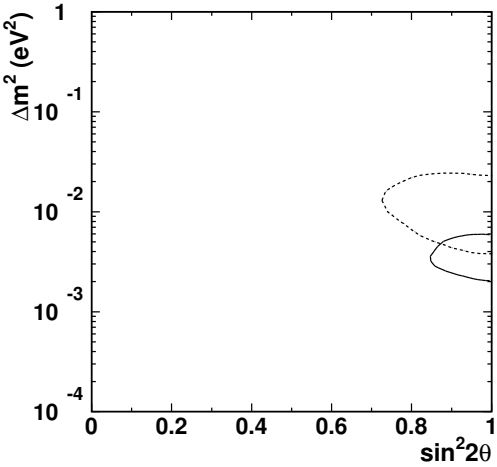

Figure 4. The allowed parameter region of $\nu_\mu \leftrightarrow \nu_\tau$ neutrino oscillations by a combined analysis of FC, PC, upward stopping muon and upward through-going muon events from Super-Kamiokande (solid curve, preliminary). Result from Kamiokande by a similar analysis (without the upward stopping muon data) is also shown (dashed curve).

3. Solar neutrinos

The Sun is an intense source of low-energy electron neutrinos which are products of the nuclear processes in its central region. Neutrinos from the $^8B \rightarrow ^8 Be^* + e^+ + \nu_e$ reaction (^{8}B solar neutrinos) are observed in Super-Kamiokande. The uncertainty of the calculated flux of ^{8}B solar neutrinos is $^{+19}_{-14}\%$ [15], largely due to the uncertainty in the reaction rate of $^7Be + p \rightarrow ^8 B + \gamma$.

Five solar neutrino experiments, Homestake [16], Kamiokande [17], SAGE [18], GALLEX [19] and Super-Kamiokande [20], confirmed the basic mechanism of the energy generation in the Sun. However, the observed fluxes from all the solar neutrino experiments were lower than the Standard Solar Model (SSM) predictions. It is widely known that it is extremely difficult to consistently explain all the data in the context of solar physics.

3.1. Tests of solar neutrino oscillations

The MSW mechanism [21] or the vacuum neutrino oscillations can explain all the existing solar neutrino data naturally. For the definite confirmation of solar neutrino oscillations, we need experimental results which can not be predicted by any solar models. Furthermore, we need to know the parameter region of neutrino oscillations. It is predicted that the spectrum of the ^{8}B solar neutrinos should be distorted significantly for the cases of the "small angle MSW solution" and the "vacuum oscillation solution", or the day-night effect should be observed for a region of the "large mixing MSW solution".

Super-Kamiokande provides the information for both the energy spectrum and the day-night effect. Super-Kamiokande detects ^{8}B solar neu-

[3] For the definition of χ^2, see Ref. [14].

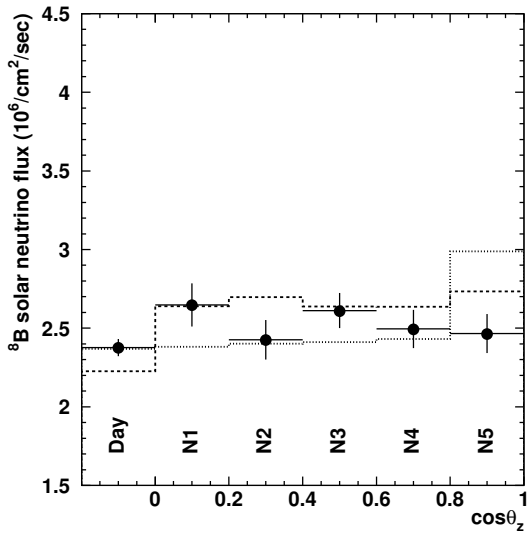

Figure 5. Day-night data from Super-Kamiokande. The night time data are subdivided into five bins (N1∼N5) according to the angle between the direction to the Sun and the nadir at the detector. The dashed and dotted histograms show the expected day-night effect for (Δm^2, sin$^2 2\theta$) = (1.2×10^{-5}eV^2, 0.56) and (6.3×10^{-6} eV^2, 0.01), respectively. These points are excluded at 99%C.L..

trinos through neutrino-electron scattering, $\nu e \rightarrow \nu e$. The electron energy, direction and the time of the reaction are measured. The energy scale, the energy resolution, the angular resolution and the vertex position resolution were calibrated mainly based on the electron beam of 5∼16MeV from a LINAC system. The absolute energy scale was understood within 0.6 % in this energy range.

The measured ^{8}B solar ν_e flux above 6.5 MeV during 825 days of the observation time was 2.45 $\pm$0.04(stat.) $\pm$0.07(sys.) $\times10^6$/cm^2/sec, which was 0.475 $^{+0.008}_{-0.007}$(stat.) $\pm$0.013(sys. of the data) of the SSM prediction [15]. Solar neutrino events in a lower energy region (5.5 to 6.5 MeV) were also observed (524 days of data). The observed flux in this energy range was consistent with the higher energy data, see Figure 6.

Figure 5 shows the day-night data from Super-Kamiokande. The data were expressed as: $Night/Day$ = 1.067$\pm$0.033(stat.)$\pm$0.013(sys.). The possible excess of the flux in the night time was only a 2 σ effect and was not conclusive yet.

Figure 6 shows the energy spectrum of the recoil-electrons from Super-Kamiokande divided by the SSM prediction. The Data/SSM values in the end-point region were higher than the average. The statistical significance of the possible distortion of the energy spectrum was tested by a χ^2 method. The absolute flux value was assumed to be a free parameter and only the shape of the data and the expectations was compared. The χ^2 values were obtained to be 24.3, 25.0 and 17.4 (DOF=17) for the no distortion case (i.e., no oscillation effect), a small mixing case ($\sin^2 2\theta = 5\times10^{-3}$, $\Delta m^2 = 5\times10^{-6}$eV^2) and the best fit in the vacuum oscillation solution ($\sin^2 2\theta$ =0.79, $\Delta m^2 = 4.3\times10^{-10}$eV^2), respectively. The vacuum oscillation gave the smallest χ^2 value. But, we would like to comment that the confidence level of disfavoring the flat Data/SSM distribution in energy is weaker than that with 500 days of data [20]. Thus the energy spectrum measurement was not conclusive. We need more data for further understanding of the solar neutrino problem.

4. Summary

After reporting the evidence for neutrino oscillations in 1998, Super-Kamiokande has significantly increased the statistics of the atmospheric neutrino data. With the updated data, the main feature of the data was essentially the same: Both the zenith angle distribution of μ-like events and the (μ/e) values were significantly different from the predictions in the absence of neutrino oscillations. While uncertainties in the flux prediction, cross sections, and experimental biases were ruled out as explanations of the observations, the data were in good agreement with two-flavor $\nu_\mu \leftrightarrow \nu_\tau$ oscillations. This conclusion was supported by the upward-going muon results. By using all the atmospheric neutrino data from Super-Kamiokande, we calculated the 90% C.L. allowed region of neutrino oscillation parameters: $2\times10^{-3} < \Delta m^2 < 6\times10^{-3}$eV^2 and $\sin^2 2\theta > 0.84$. With these updated data, we conclude that the

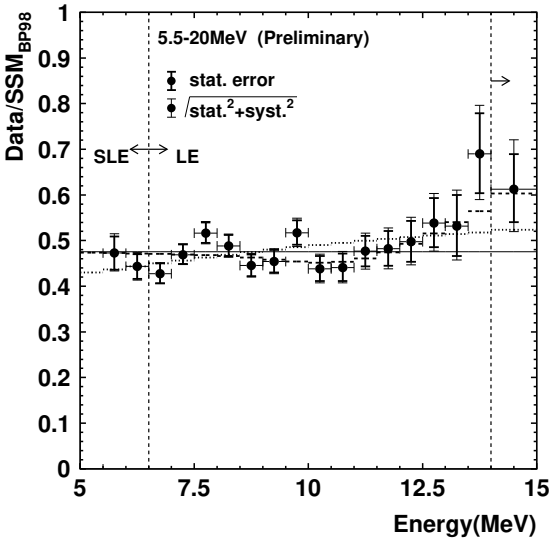

Figure 6. Plot of Data/SSM as a function of electron energy from Super-Kamiokande. The inner error bars are statistical and the outer error bars are total errors with statistical and systematic errors added in quadrature. The dotted and dashed histograms show the expected energy spectrum for a typical small-mixing solution ($\sin^2 2\theta = 5 \times 10^{-3}$, $\Delta m^2 = 5 \times 10^{-6}\mathrm{eV}^2$) and the best-fit vacuum-oscillation solution ($\sin^2 2\theta$ =0.79, $\Delta m^2 = 4.3 \times 10^{-10}\mathrm{eV}^2$), respectively.

evidence for neutrino oscillations is much stronger now.

All the solar neutrino data, including those from Super-Kamiokande, showed the deficit of solar neutrinos relative to the SSM predictions. The data can be explained by either the "small-mixing MSW solution", "large-mixing MSW solution" or "vacuum oscillation solution". We tried to distinguish the solutions by studying the day-night effect and the energy spectrum of ^{8}B solar neutrinos. The present Super-Kamiokande data did not distinguish the three solutions. More data are required for further understanding of the solar neutrino problem.

REFERENCES

1. K.S.Hirata, *et al.*, Phys. Lett. B, **205** (1988) 416; **280** (1992) 146.
2. Y.Fukuda, *et al.*, Phys. Lett. B, **335** (1994) 237.
3. D.Casper, *et al.*, Phys. Rev. Lett., **66** (1991) 2561; R.Becker-Szendy, *et al.*, Phys. Rev. D, **46** (1992) 3720.
4. W.W.M.Allison, *et al.*, Phys. Lett. B, **391** (1997) 491; **449** (1999) 137.
5. M.Apollonio, *et al.*, Phys. Lett. B, **420** (1998) 397; hep-ex/9907037.
6. Y.Fukuda, *et al.*, Phys. Lett. B, **433** (1998) 9; **436** (1998) 33.
7. Y.Fukuda, *et al.*, Phys. Rev. Lett., **81** (1998) 1562.
8. M.Gluck, E.Reya and A.Vogt, Z. Phys. C, **67** (1995) 433.
9. Y.Fukuda, *et al.*, Phys. Rev. Lett, **82** (1999) 2644.
10. G.Barr, *et al.*, Phys. Rev. D, **39** (1989) 3532; V.Agrawal, *et al.*, Phys. Rev. D, **53** (1996) 1313.
11. M.Honda, *et al.*, Phys. Lett. B, **248** (1990) 193; Phys. Rev. D, **52** (1995) 4985.
12. S.Hatakeyama, *et al.*, Phys. Rev. Lett., **81** (1998) 2016.
13. Y.Fukuda, *et al.*, submitted for publication to Phys. lett. B; hep-ex/9908049.
14. The Super-Kamiokande collaboration, draft in preparation.
15. J.N.Bahcall, S.Basu, and M.H.Pinsonneault, Phys. Lett. B, **433** (1998) 1.
16. B.T.Cleveland, *et al.*, Astrophys.J., **496** (1998) 505.
17. Y.Fukuda, *et al.*, Phys. Rev. Lett., **77** (1996) 1683.
18. J.N.Abdurashitov, *et al.*, Phys. Rev. Lett. B, **77** (1996) 4708; astro-ph/9907131.
19. W.Hampel, *et al.*, Phys. Lett. B, **447** (1999) 127.
20. Y.Fukuda, *et al.*, Phys. Rev. Lett., **81** (1998) 1158; **82** (1999) 1810; **82** (1999) 2430.
21. L.Wolfenstein, Phys. Rev. D, **17** (1978) 2369; S.P.Mikheyev and A.Yu.Smirnov, Sov. J. Nucl. Phys., **42** (1985) 1441; Nuovo Cim. C, **9** (1986) 17.